



## Oxidation of perchloroethylene—Activity and selectivity of Pt, Pd, Rh, and V<sub>2</sub>O<sub>5</sub> catalysts supported on Al<sub>2</sub>O<sub>3</sub>, Al<sub>2</sub>O<sub>3</sub>-TiO<sub>2</sub> and Al<sub>2</sub>O<sub>3</sub>-CeO<sub>2</sub>

Satu Pitkäaho <sup>a,\*</sup>, Lenka Matejova <sup>b</sup>, Satu Ojala <sup>a</sup>, Jana Gaalova <sup>b</sup>, Riitta L. Keiski <sup>a</sup>

<sup>a</sup> University of Oulu, Department of Process and Environmental Engineering, P.O. Box 4300, FI-90014 University Of Oulu, Finland

<sup>b</sup> Institute of Chemical Process Fundamentals of the ASCR, v.v.i., Department of Catalysis and Reaction Engineering, Rozvojová 135, 165 02 Prague 6, Czech Republic

### ARTICLE INFO

#### Article history:

Received 18 July 2011

Received in revised form

15 November 2011

Accepted 18 November 2011

Available online 28 November 2011

#### Keywords:

Catalytic oxidation

Chlorinated volatile organic compounds

CVOC

Perchloroethylene

Tetrachloroethylene

Tetrachloroethene

Emission abatement

### ABSTRACT

The total oxidation of perchloroethylene (PCE) over Pt, Pd, Rh and V<sub>2</sub>O<sub>5</sub> metallic monolith catalysts supported on Al<sub>2</sub>O<sub>3</sub> as well as CeO<sub>2</sub> and TiO<sub>2</sub>-doped Al<sub>2</sub>O<sub>3</sub> was examined. To ensure high HCl yields, the amount of water as a hydrogen source was optimized to be 1.5 wt-% by testing the effect of water content on PCE oxidation. Water not only enhanced the selectivity towards HCl formation but also improved the PCE oxidation to some extent.

Both, the activity and selectivity of the catalysts were found to be related to the properties of the catalyst support; addition of TiO<sub>2</sub> or CeO<sub>2</sub> into Al<sub>2</sub>O<sub>3</sub> enhanced catalysts' efficiency regardless of the active phase. Pt, Pd and Rh catalysts showed high catalytic activity, PCE conversions ranging from 72% to 99%, and HCl yields from 59% up to 93% were observed. Both activity and selectivity of the Pt/Al<sub>2</sub>O<sub>3</sub>-CeO<sub>2</sub> and Pd/Al<sub>2</sub>O<sub>3</sub>-CeO<sub>2</sub> catalysts were superior to the other tested catalysts. The results show that over the oxidation of PCE, the redox properties of the catalyst and the amount of activated oxygen may play bigger role than the acidity. To confirm the suspected positive effect on the PCE oxidation coming from the bidispersed mesopores seen over ceria-doped catalysts needs further testing.

© 2011 Elsevier B.V. All rights reserved.

### 1. Introduction

In Europe three most commonly used chlorinated hydrocarbons are dichloromethane (DCM), perchloroethylene (PCE) and trichloroethylene (TCE) [1]. Of these three commonly used chemicals PCE (C<sub>2</sub>Cl<sub>4</sub>) was chosen as a model compound, since PCE oxidation is not widely studied and it is present in industrial emissions as mixtures with other compounds. PCE is specified as an eye and skin irritating chemical known to damage liver, kidneys, central nervous system and is suspected to be a human carcinogen [2]. In the International Chemical Safety Cards [3] PCE is defined to be 'toxic to aquatic organisms, may cause long-term adverse effects in the aquatic environment'.

Due to their harmful properties e.g. in EU the release of CVOCs is controlled by strict regulations [4], which are setting high demands for CVOC abatement systems. The methods of reducing VOC emissions resulting from solvent use can be grouped into three broad categories: process modifications including the improvement of management practices, solvent substitutions aiming at reduced solvent use and add-on technologies which are appropriate for 'enclosed' operations where solvents can be captured. Among the add-on technologies, low temperature catalytic oxidation can

economically destroy the pollutants instead of only removing them from gas for recycling them elsewhere in the biosphere [5–7].

In general, the catalysts applied in the CVOC destruction should be highly active, maintain high resistance towards deactivation by chlorine and its compounds and have high selectivity towards CO<sub>2</sub> and HCl formation. The reactivity of CVOCs in the catalytic oxidation, as well as the distribution of the reaction products, depends strongly on the used catalyst and the chemical structure of the oxidized compounds [8–10]. Earlier studies on CVOCs oxidation over different types of catalysts show that noble metal catalysts are more selective and active than metal-oxide-based catalysts or perovskites. Besides the active compound, destruction of CVOCs strongly depends on the catalyst support [8–23].

Among the large number of CVOCs, those compounds containing more chlorine atoms than hydrogen atoms, cannot be totally converted by air to the most desirable chlorine-containing product i.e. HCl. In these cases even more toxic products such as chlorine (due to Deacon reaction) and phosgene (COCl<sub>2</sub>) can be formed. To improve selectivity towards HCl, either a hydrogen-rich organic additive or water vapor should be added to the feed stream. It has been reported that the presence of water, not only promotes the selectivity towards environmentally desirable reaction products, HCl and CO<sub>2</sub>, but also often affects positively the CVOC conversion [6,8–10,12,24]. PCE is an unsaturated C<sub>2</sub> compound containing four chlorine atoms and a carbon–carbon double bond, which makes the compound very difficult to be completely oxidized since

\* Corresponding author. Tel.: +358 8 553 2374; fax: +358 8 553 2304.

E-mail address: [satu.pitkaaho@oulu.fi](mailto:satu.pitkaaho@oulu.fi) (S. Pitkäaho).

unsaturated CVOCs are more stable than the saturated ones [11,16–18,24]. Since there is no hydrogen in PCE, special attention needs to be paid to the by-product formation.

The objective of this study was to test the activity and selectivity of Pt, Pd, Rh and V<sub>2</sub>O<sub>5</sub> on three different washcoats, Al<sub>2</sub>O<sub>3</sub>, Al<sub>2</sub>O<sub>3</sub>-TiO<sub>2</sub> and Al<sub>2</sub>O<sub>3</sub>-CeO<sub>2</sub> on metallic monolithic supports in PCE oxidation. The catalysts were characterized by ICP-OES (inductively coupled plasma optical emission spectroscopy), chemisorption, physisorption (BET, BJH), XRD, UV-vis DRS, isotopic exchange and ion chromatography. The aim was to find the most favorable properties of the catalysts so that even more efficient and environmentally friendly catalysts could be developed for the catalytic abatement of CVOCs. Before starting the activity tests different water concentrations were tested to optimize the oxidation conditions.

## 2. Experimental

### 2.1. Catalysts

The catalysts used were metallic monoliths (manufactured by Ecocat Oy) with the cell density of 500 cpsi [24]. Three different washcoats (Al<sub>2</sub>O<sub>3</sub>, Al<sub>2</sub>O<sub>3</sub>-TiO<sub>2</sub> and Al<sub>2</sub>O<sub>3</sub>-CeO<sub>2</sub>) and four different active phases (Pt, Pd, Rh and V<sub>2</sub>O<sub>5</sub>) were used to prepare all together fifteen (15) catalysts (12 with active phase). The weight ratio of the Al<sub>2</sub>O<sub>3</sub>:TiO<sub>2</sub> washcoat was equal to 3:1. Similar composition with Al<sub>2</sub>O<sub>3</sub>:CeO<sub>2</sub> was used. The washcoats were prepared so that the initial washcoat slurry contained the two given oxides. The amount of support on the metal foil was set to be constant, being 24% of the total weight of the catalyst. In order to reach comparability between noble metal catalysts the noble metal loading was fixed by the moles (*n*) and therefore the targeted catalyst loadings on the washcoats were 1% with Pt catalysts and 0.5% with Pd and Rh catalysts. With vanadium catalysts the targeted V<sub>2</sub>O<sub>5</sub> loading was 5%. Used precursor salts were Pd(NH<sub>3</sub>)<sub>4</sub>(NO<sub>3</sub>)<sub>2</sub>, Rh(NO<sub>3</sub>)<sub>3</sub>, Pt(NH<sub>3</sub>)<sub>4</sub>(HCO<sub>3</sub>)<sub>2</sub> and V<sub>2</sub>C<sub>2</sub>O<sub>4</sub>. After the post-impregnation of the active phase, the catalysts were calcined at 550 °C for 4 h. Actual characteristics of the tested catalyst and supports are presented in more detail in Tables 1 and 2.

### 2.2. Catalyst characterization

If not stated otherwise, the catalyst characterization was performed on the catalysts in their manufactured state as described in Section 2.1.

The active metal contents of the catalysts were analyzed by using microwave-assisted sample digestion and ICP-OES determination using PerkinElmer Optima 5300 DV. The analysis was done on a powder form of Pt, Pd, Rh and V<sub>2</sub>O<sub>5</sub> catalysts scraped from the metallic monolith surface.

The specific surface areas (*S*<sub>BET</sub>), net pore volumes (*V*<sub>p</sub>) and pore-size distributions (PSD) were determined from nitrogen physisorption at –196 °C performed on an automated volumetric apparatus ASAP2020 Micrometrics. Before analysis, samples were degassed for 2 h at 350 °C in vacuum (2 Pa). Specific surface areas, *S*<sub>BET</sub> (m<sup>2</sup> g<sup>–1</sup>), were evaluated from adsorption data in the interval of relative adsorbate pressures *p/p*<sub>0</sub> = (0.05–0.30) according to the classical BET theory. The pore-size distributions were evaluated by the Barret, Joyner, Halenda method (BJH) based on the empirical Lecloux-Pirard standard isotherm and cylindrical pore geometry. The net pore volumes, *V*<sub>p</sub>, were determined as the adsorbed amount of nitrogen at *p/p*<sub>0</sub> = 0.99.

All dispersions of Pt, Pd and Rh, excluding Rh/Al<sub>2</sub>O<sub>3</sub>-CeO<sub>2</sub>, were determined by CO chemisorption at 35 °C using volumetric ASAP2020 Micrometrics Chemi System. Prior to CO uptake

determination, all samples were reduced under hydrogen (2 h at 350 °C) and then evacuated at 350 °C for 2 h followed by evacuation to 35 °C within 30 min to remove residual hydrogen. The adsorption stoichiometry Pt/CO = 1, Pd/CO = 1 and Rh/CO = 1 was assumed. The determination of Rh/Al<sub>2</sub>O<sub>3</sub>-CeO<sub>2</sub> dispersion was carried out for ~100 mg of powder scraped from metallic monolith surface with pulsed H<sub>2</sub> chemisorption at –85 °C. Prior to measurements the catalysts were reduced at 350 °C in a H<sub>2</sub> flow for 1 h and then flushed with Ar for 3 h. The analysis was done with gas chromatograph (GC), Gira instrumentation & systems, GC10C equipped with a TCD detector. The evaluation of dispersions was based on the same principle and stoichiometry as the above mentioned CO chemisorptions.

X-ray diffraction (XRD) was used to identify the phase composition and crystallite sizes of Al<sub>2</sub>O<sub>3</sub>, Al<sub>2</sub>O<sub>3</sub>-TiO<sub>2</sub> and Al<sub>2</sub>O<sub>3</sub>-CeO<sub>2</sub>. The analysis was done on a powder form of Pt, Pd and Rh catalysts on Al<sub>2</sub>O<sub>3</sub>-CeO<sub>2</sub> and Al<sub>2</sub>O<sub>3</sub>-TiO<sub>2</sub> and on pure Al<sub>2</sub>O<sub>3</sub>-support. The XRD patterns were recorded with Siemens D5000 diffractometer in the conventional focusing Bragg-Brentano geometry with fixed slits and without a monochromator. Ni-filtered CuK $\alpha$  radiation produced by a laboratory x-ray tube was used. The patterns were acquired in the diffraction angle range 2θ = 10–90°. For phase composition and crystallite size determination the whole powder pattern modeling method (WPPM) with the MSTRUCT program (Rietveld fitting analysis included) was used [25,26].

UV-vis diffuse reflectance spectroscopy (DRS) was used to identify the types of vanadium species on all three supports. UV-vis DRS spectra were recorded using GBS CINTRA 303 spectrometer equipped with a diffuse reflectance attachment with a spectralon-coated integrating sphere against a spectralon reference. Granulated materials (0.25–0.50 mm) were dehydrated under oxygen stream at 450 °C for 1 h, cooled to 150 °C in oxygen and followed by their evacuation at 150 °C under vacuum of 0.1 Pa for 15 min [27]. In order to receive spectra of vanadium-catalysts at lower intensity, catalyst samples were diluted with pure alumina support as reported previously [28].

Isotopic oxygen exchange activities (oxygen activation properties) of Pt-containing catalysts were examined with a temperature programmed method. The experiments were carried out in a closed-loop reactor system, where a re-circulating pump was used in order to avoid any diffusion and mass transport effects in the gas phase that affect partial pressures of different isotopomers measured continuously by mass spectrometry (Pfeiffer Vacuum). The experimental procedure was following: The needed amount of <sup>18</sup>O<sub>2</sub> (supplied by Isotec with 99.3 <sup>18</sup>O atom-% purity for <sup>18</sup>O<sub>2</sub>) was first introduced into the reactor system after which the system inlet was closed. During the introduction of the gases into the system, the entry of the actual reactor cell was closed. After the inlet concentrations of the reactants were measured, the reactor inlet was opened. The total pressure of the reacting gas was kept constant (50 mbar) in all the experiments. After opening the reactor cell, the heating rate was set to 2 °C min<sup>–1</sup> starting from ~100 °C up to ~550 °C. Prior to each experiment the catalysts were first oxidized (15 min at 550 °C), then reduced (15 min at 550 °C) and finally evacuated for ~30 min at the same temperature. The temperature of the oven was then decreased to the starting level while the catalyst was kept in vacuum. The amount of a powder form catalyst sample in one experiment was ~20 mg.

Ion chromatography (IC) was used to determine water soluble chlorine from fresh and used Pt catalysts supported on Al<sub>2</sub>O<sub>3</sub>, Al<sub>2</sub>O<sub>3</sub>-TiO<sub>2</sub> and Al<sub>2</sub>O<sub>3</sub>-CeO<sub>2</sub>. The sample for the IC test was prepared by scraping the catalyst material from the monolith surface and mixing the material with water in the 1:1 ratio at room temperature for 60 min to dissolve the probable residual chlorine from the catalyst surface. 2 mM NaHCO<sub>3</sub>/1.3 mM Na<sub>2</sub>CO<sub>3</sub> was used as an eluent in IC and the column used was Metrosep Anion Dual 2.

**Table 1**

Tested monoliths and their properties.

Catalyst	Metal loading (wt-%)	Metal dispersion (%)	Metallic surface area ( $\text{m}^2 \text{ g}^{-1}$ metal)	$S_{\text{BET}}$ ( $\text{m}^2 \text{ g}^{-1}$ )		
				Fresh	Pre-treated <sup>a</sup>	Used
Pt/Al <sub>2</sub> O <sub>3</sub>	0.97	49.4	121.9	140.1	132.6	111.0
Pd/Al <sub>2</sub> O <sub>3</sub>	0.72	16.2	72.1	152.0	n.d.	98.1
Rh/Al <sub>2</sub> O <sub>3</sub>	0.59	29.0	127.5	162.8	n.d.	103.8
V/Al <sub>2</sub> O <sub>3</sub>	5.7	n.d.	n.d.	169.5	n.d.	99.7
Pt/Al <sub>2</sub> O <sub>3</sub> -TiO <sub>2</sub>	1.3	49.8	123.0	127.5	103.6	79.9
Pd/Al <sub>2</sub> O <sub>3</sub> -TiO <sub>2</sub>	0.64	19.5	87.1	140.5	n.d.	104.0
Rh/Al <sub>2</sub> O <sub>3</sub> -TiO <sub>2</sub>	0.71	61.0	268.4	163.0	n.d.	120.5
V/Al <sub>2</sub> O <sub>3</sub> -TiO <sub>2</sub>	5.2	n.d.	n.d.	144.2	n.d.	111.1
Pt/Al <sub>2</sub> O <sub>3</sub> -CeO <sub>2</sub>	1.3	35.5	87.6	160.5	131.3	97.4
Pd/Al <sub>2</sub> O <sub>3</sub> -CeO <sub>2</sub>	0.61	32.6	145.0	151.3	n.d.	95.9
Rh/Al <sub>2</sub> O <sub>3</sub> -CeO <sub>2</sub>	0.55	74.9	332.7	170.6	n.d.	103.1
V/Al <sub>2</sub> O <sub>3</sub> -CeO <sub>2</sub>	5.4	n.d.	n.d.	148.3	n.d.	112.8

n.d. = not determined.

<sup>a</sup> Pretreatment in air flow from RTP to 700 °C (or to 600 °C with vanadium catalysts).

HSC Chemistry Software was used to calculate the enthalpy for one PCE component at room temperature in order to see the theoretical differences between bond energies of the atoms in the PCE molecule. This method is only the estimation of what might happen since the calculated bond energies are averages, but still some evaluation e.g. about possible by-products could be done based on these calculations.

### 2.3. Activity experiments

The activity experiments were carried out in a tubular quartz reactor operating under atmospheric pressure. Due to corrosive reaction products, all the materials used in the experimental set-up are corrosion resistant: quartz glass, heated Teflon piping ( $T = 180^\circ\text{C}$ ) and Teflon connectors. In the vaporizer unit liquid VOC and water were fed with syringe pumps equipped with gas tight syringes to the heater for vaporization and to be mixed with air coming from a mass flow controller. The preheating oven, filled with glass spheres to ensure the mixing of gases, was set to 150 °C. The reaction temperature was measured outside the reactor right before the monolith and then corrected to represent the value inside the reactor.

The gas analysis during the experiments was carried out with the Gasmet DX-4000N FTIR analyzer, which is able to measure almost all gas phase compounds excluding noble gases and diatomic homonuclear compounds such as O<sub>2</sub>, N<sub>2</sub>, Cl<sub>2</sub>. The analyzer was calibrated to detect the following chlorinated hydrocarbons: C<sub>2</sub>Cl<sub>4</sub>, C<sub>2</sub>HCl<sub>3</sub>, CH<sub>3</sub>Cl, CH<sub>2</sub>Cl<sub>2</sub>, CHCl<sub>3</sub>, COCl<sub>2</sub> and HCl. The analyzer consists of a high temperature sample cell, a temperature controlled and peltier cooled MCT-detector, and signal processing electronics. Calcmet for Windows analysis software was used to analyze the spectra. Due to the analysis, the complete closing of the chlorine-balance is not possible, since the formation of Cl<sub>2</sub> was not measured. The selectivity towards HCl, the desired oxidation product, was followed by measuring the HCl concentration at the outlet and calculating the HCl yield in the following way:

$$Y_{\text{HCl}} = 100 \times \frac{C_{\text{HCl}}^{\text{out}}}{4 \times C_{\text{PCE}}^{\text{in}}} \quad (1)$$

where  $Y_{\text{HCl}}$  is the HCl yield [%],  $C_{\text{HCl}}^{\text{out}}$  is the measured HCl concentration [ppm] and  $C_{\text{PCE}}^{\text{in}}$  is the feed concentration of PCE [ppm].

The PCE (C<sub>2</sub>Cl<sub>4</sub>, Algol, 99.0 area-%) concentration was 500 ppm in all tests. Prior to light-off experiments, to determine the optimal amount of additional water to be used to ensure the sufficient selectivity towards HCl, steady state tests at 600 °C with one of the platinum catalysts, Pt/Al<sub>2</sub>O<sub>3</sub>-CeO<sub>2</sub>, were done with various water concentrations; 0.3 wt-%, 0.7 wt-%, 1.1 wt-%, 1.6 wt-%, 2 wt-% and 3 wt-%. As a result, all activity tests were performed in the presence of 1.5 wt-% water. The flow of the reaction mixture was set to be 1.07 l min<sup>-1</sup> amounting to gas hourly space velocity (GHSV) of 32 000 h<sup>-1</sup> during all experiments. The reaction temperature ranged from 100 °C to 700 °C (to 600 °C with vanadium containing catalysts) and the heating rate used was 10 °C min<sup>-1</sup>. Before every test, pre-treatment of the catalysts was done in an air flow by heating up the catalyst from room temperature to 700 °C (or to 600 °C with vanadium catalysts) and then cooling it down to room temperature (or 100 °C) in air flow. Activity tests were carried out over all catalysts (12) as well as over all three supports. The light-off tests were repeated at least once to verify the results.

## 3. Results

### 3.1. Properties of the catalysts

Specific surface areas were measured for all the metal-doped catalysts before and after the tests. These results together with metal loadings and dispersions of noble metals are listed in Table 1. The metal dispersion was the lowest for Pt and the highest for Pd over the Al<sub>2</sub>O<sub>3</sub>-CeO<sub>2</sub> supported catalysts, 35.5% and 32.6%, respectively. With the Rh catalysts the metal dispersion was significantly high over both titania and ceria-doped catalysts; the Rh dispersions were more than double when compared to alumina supported catalysts. In general, the specific surface areas ( $S_{\text{BET}}$ ) of the fresh reference supports did not differ a lot from each other as the surface areas range from 134 to 172 m<sup>2</sup> g<sup>-1</sup> (Table 2). The  $S_{\text{BET}}$  of all tested catalysts were observed to decrease significantly after the PCE oxidation tests, from 21% to 41% decrease

**Table 2**Textural properties of Al<sub>2</sub>O<sub>3</sub>, Al<sub>2</sub>O<sub>3</sub>-TiO<sub>2</sub> and Al<sub>2</sub>O<sub>3</sub>-CeO<sub>2</sub> supports and the surface area of clean metal foil.

Reference support	$S_{\text{BET}}$ ( $\text{m}^2/\text{g}$ )	$V_p$ ( $p/p_0 = 0.990$ ) ( $\text{mm}^3 \text{ liq/g}$ )	PSD type	Mesopore size (nm)
Al <sub>2</sub> O <sub>3</sub> <sup>a</sup>	172.1	430	Mono-	7.7
Al <sub>2</sub> O <sub>3</sub> -TiO <sub>2</sub> <sup>a</sup>	134.8	370	Mono-	7.8
Al <sub>2</sub> O <sub>3</sub> -CeO <sub>2</sub> <sup>a</sup>	165.7	356	Bi-	3.6 and 7.5
Metallic foil	0.21 <sup>KR</sup>	–	–	–

<sup>a</sup> Parameters were measured for powder catalysts.

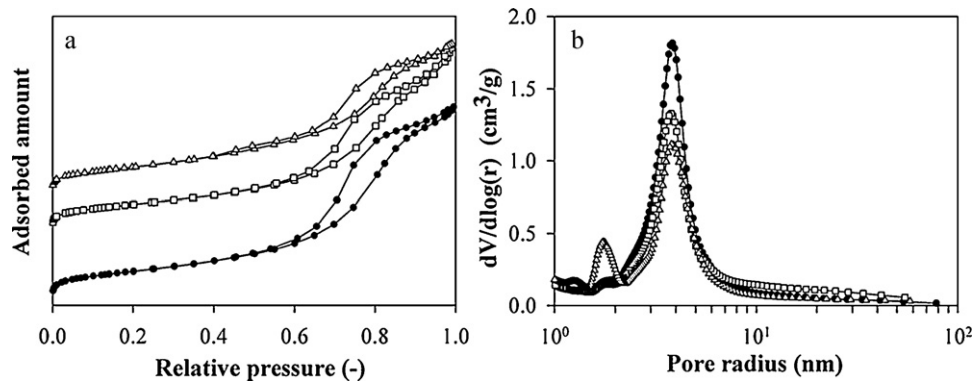


**Fig. 1.** (a) Nitrogen adsorption–desorption isotherms at  $-196^{\circ}\text{C}$  and (b) pore-size distributions of the Pt catalysts ( $\bullet$   $\text{Pt}/\text{Al}_2\text{O}_3$ ,  $\square$   $\text{Pt}/\text{Al}_2\text{O}_3\text{-TiO}_2$ ,  $\triangle$   $\text{Pt}/\text{Al}_2\text{O}_3\text{-CeO}_2$ ) (the isotherms of  $\text{Pt}/\text{Al}_2\text{O}_3\text{-TiO}_2$  and  $\text{Pt}/\text{Al}_2\text{O}_3\text{-CeO}_2$  were shifted up to improve the visibility).

in surface areas were seen (Table 1), and therefore the surface areas for the platinum catalysts were also measured after the pre-treatment procedure (see Section 2.3). It was indeed seen that the used pre-treatment is responsible for about 50% of the surface area loss with the  $\text{TiO}_2$  and  $\text{CeO}_2$ -doped catalysts and about 30% with the  $\text{Al}_2\text{O}_3$  supported catalysts. This decrease in  $S_{\text{BET}}$  was actually expected since fresh catalysts were calcined at  $550^{\circ}\text{C}$  and the pre-treatment temperature with Pt catalysts was raised up to  $700^{\circ}\text{C}$ .

Nitrogen adsorption–desorption isotherms of Pt catalysts at  $-196^{\circ}\text{C}$  show typical I+IV types of adsorption isotherms (according to the IUPAC classification) corresponding to mesoporous structure of the support with a small amount of micropores (Fig. 1a) [29]. However, some evident differences between the supports can be seen. The desorption branch of the  $\text{Al}_2\text{O}_3\text{-CeO}_2$  isotherm joins to its adsorption branch at lower relative pressure ( $p/p_0 = 0.40$ ) than in the  $\text{Al}_2\text{O}_3$  and  $\text{Al}_2\text{O}_3\text{-TiO}_2$  isotherms ( $p/p_0 = 0.55$ ). This result corresponds to the existence of smaller mesopores in the  $\text{Al}_2\text{O}_3\text{-CeO}_2$  support, which is clearly visible in the evaluated pore-size distribution curves shown in Fig. 1b. Textural properties of  $\text{Al}_2\text{O}_3$ ,  $\text{Al}_2\text{O}_3\text{-TiO}_2$ , and  $\text{Al}_2\text{O}_3\text{-CeO}_2$  catalysts without the active phase are summarized in Table 2.

According to the measured XRD pattern of  $\text{Al}_2\text{O}_3$ , the presence of  $\gamma$ -alumina was confirmed. However, the  $\text{Al}_2\text{O}_3$  crystallite size was not determined since the materials under study are nano-sized crystals with a high defect frequency in crystal lattice (mainly  $\gamma$ -alumina) far from the ideal crystals [30]. There is a notable peak overlap of  $\gamma$ -alumina/ceria and  $\gamma$ -alumina/titania in the spectra (Fig. 2). In the alumina mixed with ceria one individual peak exists and in the mixture with titania two ‘not-overlapping peaks’ appear, but since all three catalysts (Pt, Pd and Rh on each support) gave the same quantitative results, the weight ratios with crystallite sizes for the Pt catalysts are presented in Table 3. Evaluated weight ratios over both  $\text{Al}_2\text{O}_3\text{:TiO}_2$  and  $\text{Al}_2\text{O}_3\text{:CeO}_2$  washcoats confirm the weight ratios of 3:1 that was the target during the catalyst preparation by the manufacturer. Due to low concentration of all metals (Pt, Pd, Rh) no conclusion about their crystallinity could be withdrawn based on XRD. Since vanadium catalysts did not show any diffraction peaks typical to crystalline  $\text{V}_2\text{O}_5$ , further characterization with UV-vis diffuse reflectance spectroscopy over vanadium catalysts was performed.

UV-vis DRS characterization confirmed that crystalline  $\text{V}_2\text{O}_5$  did not exist on any of the supports. In all samples tetrahedrally (Td) and octahedrally (Oh) coordinated vanadium species were observed. Over  $\text{Al}_2\text{O}_3\text{-TiO}_2$  the population of Td-coordinated vanadium in monomers and oligomers was higher whereas over  $\text{Al}_2\text{O}_3$  and  $\text{Al}_2\text{O}_3\text{-CeO}_2$  supports higher population of Oh-coordinated vanadium in 3D polymeric species was detected. The exact

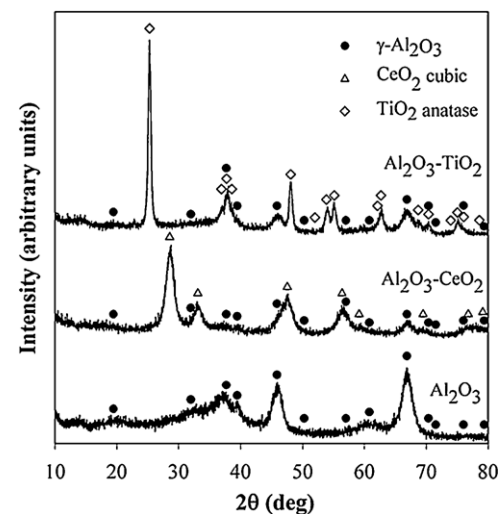


**Fig. 2.** XRD patterns of  $\text{Al}_2\text{O}_3$ ,  $\text{Al}_2\text{O}_3\text{-CeO}_2$  and  $\text{Al}_2\text{O}_3\text{-TiO}_2$  supports.

quantification of Td- and Oh-coordinated vanadium species was unsuccessful due to high sample dilution [28]. For partial oxidation of hydrocarbons, thin vanadium layers are found to be more active and selective than  $\text{V}_2\text{O}_5$  crystallites. Furthermore, the V–O–M (M is the cation of the support) bond to the support are assumed to be crucial to the reducibility and acid-phase properties of the catalysts [31–33].

Results of temperature programmed isotopic oxygen exchange experiments for the studied Pt catalysts are shown in Fig. 3. Results

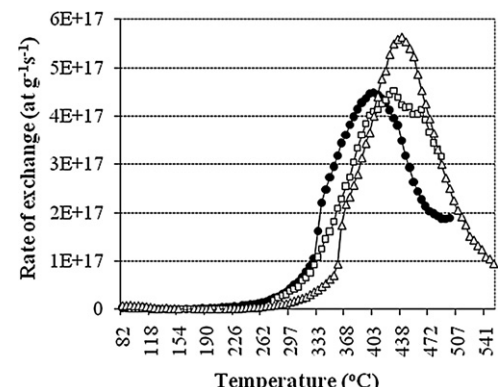


**Fig. 3.** Comparison of oxygen activation measured by isotopic exchange at different temperatures over the Pt catalysts,  $\text{Al}_2\text{O}_3$   $\bullet$ ,  $\text{Al}_2\text{O}_3\text{-TiO}_2$   $\square$ ,  $\text{Al}_2\text{O}_3\text{-CeO}_2$   $\triangle$ .

**Table 3**

Structural properties and phase compositions of Pt catalyst supported on  $\text{Al}_2\text{O}_3$ ,  $\text{Al}_2\text{O}_3\text{-TiO}_2$  and  $\text{Al}_2\text{O}_3\text{-CeO}_2$ .

Reference support	XRD		Crystallite size (nm)
	Phase composition	Weight ratios (wt-%)	
$\text{Al}_2\text{O}_3$	$\gamma\text{-Al}_2\text{O}_3$	100	n.d.
$\text{Al}_2\text{O}_3\text{-TiO}_2$	$\gamma\text{-Al}_2\text{O}_3$ $\text{TiO}_2$ anatase	74 26	n.d. ~15
$\text{Al}_2\text{O}_3\text{-CeO}_2$	$\gamma\text{-Al}_2\text{O}_3$ $\text{CeO}_2$ cubic	77 23	n.d. ~5

Parameters were measured for powder catalysts.

of the experiments show that oxygen activation over  $\text{Pt}/\text{Al}_2\text{O}_3$ ,  $\text{Pt}/\text{Al}_2\text{O}_3\text{-TiO}_2$ , and  $\text{Pt}/\text{Al}_2\text{O}_3\text{-CeO}_2$  starts at 250 °C, 267 °C, and 270 °C, respectively. The maximum rate of oxygen activation was achieved at 403 °C, 428 °C and 438 °C in the same order. The addition of  $\text{CeO}_2$  increased the oxygen activation rate on the Pt catalyst, even though the maximum rate was achieved at higher temperature than over  $\text{Pt}/\text{Al}_2\text{O}_3$  and  $\text{Pt}/\text{Al}_2\text{O}_3\text{-TiO}_2$  catalysts. It is important to notice that the differences in the exchange rates between the catalysts cannot be evaluated accurately since the oxygen activation rate was calculated from a tangent of the concentration curve and as the total concentration of  $^{18}\text{O}_2$  in the gas-phase affects the rate of exchange values, especially at higher temperatures, were affected by the consumption of  $^{18}\text{O}_2$  by the reaction at lower temperatures [34]. From the IC measurements, it was seen that after the activity tests the catalysts contained water soluble chlorine from 2.7 to 4.9 mg g<sup>-1</sup>.

Based on the HSC Chemistry enthalpy calculations the average of total energy needed to direct decomposition of PCE at room temperature is 1931 kJ. The breakage of carbon–chlorine bond in the beginning at the first step requires an average of 324 kJ of energy but instead if the carbon–carbon double bond would break the energy needed is 465 kJ. After the breakage of the first chlorine anion, breaking the carbon–carbon double bond at the second stage would require 538 kJ and at the third stage it would already require 733 kJ. Based on the calculations, during each step of PCE decomposition the energy to detach chlorine is always lower than breaking the carbon–carbon double bond. Therefore, depending on the catalysts selectivity and due to introduction of excess hydrogen to the tests e.g. trichloroethylene ( $\text{C}_2\text{HCl}_3$ ) and ethylene ( $\text{C}_2\text{H}_4$ ) could be formed as intermediates during the oxidation of PCE.

### 3.2. Effect of water feed concentration

Before starting the activity experiments, the addition of 0.3 wt-%, 0.7 wt-%, 1.1 wt-%, 1.6 wt-%, 2 wt-% and 3 wt-% of water was tested to find out the proper amount of water to be added to the reaction stream to act as a hydrogen source during the activity tests. The difference in the selectivity towards HCl was evident as the HCl yield increased from 57% up to 79% as the water amount was increased from 0.3 wt-% to 3 wt-% (Fig. 4). In addition to the increased formation of HCl, also the PCE conversion was enhanced from 77% to 84%. The selectivity towards CO was not influenced by the increased amount of water since the CO concentration stayed pretty much stable at 4 ppm during the whole test.

### 3.3. Activity

To examine the effect of the support on the PCE removal the activities of catalysts with and without active phase were investigated. The PCE conversion curves of all the tested catalysts are shown in Fig. 5a–c, and the  $T_{50}$  and  $T_{90}$  temperatures are listed in Table 4. The results show that the support itself is quite active in PCE destruction and the nature of the support has a clear effect on the

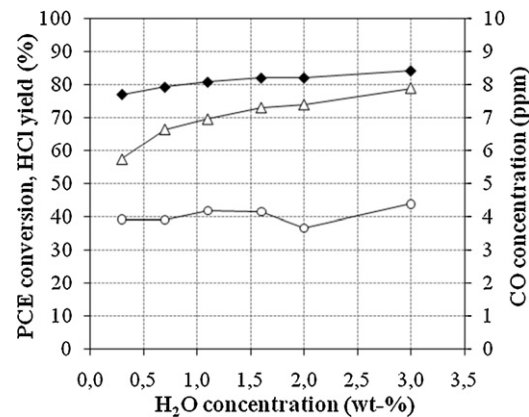


**Fig. 4.** The effect of water volume on the PCE oxidation, HCl and CO selectivity (measured  $\text{CO}_2$  concentration was 0.13 vol.% during the whole test), PCE  $\blacklozenge$ , HCl  $\triangle$ , CO  $\circ$  (PCE 500 ppm, constant temperature of 600 °C, GHSV 32 000 h<sup>-1</sup>).

activity. The overall activity order of different supports without any active phase was  $\text{Al}_2\text{O}_3\text{-CeO}_2 > \text{Al}_2\text{O}_3\text{-TiO}_2 > \text{Al}_2\text{O}_3$  as the light-off ( $T_{50}$ ) temperatures were 617 °C, 660 °C and 684 °C, respectively.

The active materials used in this study were Pt, Pd, Rh and  $\text{V}_2\text{O}_5$  (Table 1) and addition of active phase to the catalyst showed substantial enhancement in PCE oxidation (Fig. 5a–c, Table 4). When Pt and  $\text{V}_2\text{O}_5$  catalysts are considered, the activity order of the supports was  $\text{Al}_2\text{O}_3\text{-CeO}_2 > \text{Al}_2\text{O}_3\text{-TiO}_2 > \text{Al}_2\text{O}_3$ , the same as previously without the addition of active phase. Over Pd and Rh catalysts the activity order of supports was  $\text{Al}_2\text{O}_3\text{-TiO}_2 > \text{Al}_2\text{O}_3\text{-CeO}_2 > \text{Al}_2\text{O}_3$ .

Over the  $\text{Al}_2\text{O}_3$  supported catalysts the activity order of active materials was Rh > Pt > Pd >  $\text{V}_2\text{O}_5$  (Fig. 5a, Table 4). The total oxidation of PCE remained unattained as the highest conversion with the Rh/ $\text{Al}_2\text{O}_3$  catalyst at 688 °C was 91%. When 26 wt-% of titania was introduced into the support the activities of Pd and Rh were notably enhanced, the  $T_{50}$  temperature was lowered by 95 °C and 38 °C, respectively. Also the activity of the  $\text{V}_2\text{O}_5$  catalysts was improved as the  $T_{50}$  was now 556 °C (over the  $\text{V}_2\text{O}_5/\text{Al}_2\text{O}_3$  catalysts  $T_{50}$  was not reached before 600 °C, see Fig. 5a). With the Pt catalyst the addition of titania decreased the  $T_{50}$  temperature a little (about 5 °C) but at the upper end of the conversion curve the activity decreased and the  $T_{90}$  temperature remained unattained below 700 °C, which was the maximum temperature used in the activity tests (Fig. 5b).

**Table 4**  
 $T_{50}$  and  $T_{90}$  temperatures of tested catalysts (°C).

	$\text{Al}_2\text{O}_3$		$\text{Al}_2\text{O}_3\text{-TiO}_2$		$\text{Al}_2\text{O}_3\text{-CeO}_2$	
	$T_{50}$	$T_{90}$	$T_{50}$	$T_{90}$	$T_{50}$	$T_{90}$
–	684	–	660	–	617	–
Pt	585	–	580	–	492	600
Pd	605	–	510	610	539	627
Rh	560	676	522	628	540	637
$\text{V}_2\text{O}_5$	a	–	556	–	520	600

<sup>a</sup> 35% conversion at 597 °C.

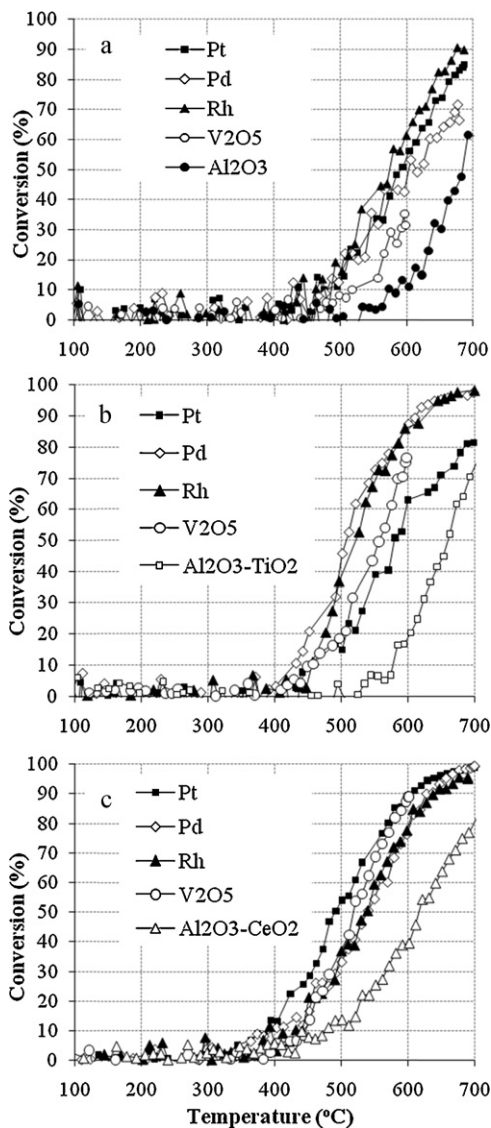


**Fig. 5.** The activity of all (a)  $\text{Al}_2\text{O}_3$  (b)  $\text{Al}_2\text{O}_3\text{-TiO}_2$  and (c)  $\text{Al}_2\text{O}_3\text{-CeO}_2$  supported catalysts (PCE 500 ppm, water 1.5 wt-%, GHSV 32 000  $\text{h}^{-1}$ ).

The activity order based on the  $T_{50}$  temperature over the  $\text{Al}_2\text{O}_3\text{-TiO}_2$  support was  $\text{Pd} > \text{Rh} > \text{V}_2\text{O}_5 > \text{Pt}$  and the highest conversion, 99% was reached with the  $\text{Rh}/\text{Al}_2\text{O}_3\text{-TiO}_2$  catalyst at 700 °C.

The addition of 23 wt-% ceria improved the catalyst activity in the cases of all active phases (Fig. 5c), the activity order of active phases was  $\text{Pt} > \text{V}_2\text{O}_5 > \text{Pd} > \text{Rh}$ , almost opposite to that over the alumina-titania support. When compared to the  $\text{Al}_2\text{O}_3$  supported catalysts, addition of ceria lowered the  $T_{50}$  temperatures of Pt, Pd and Rh by 93 °C, 66 °C and 20 °C, respectively. Over the  $\text{V}_2\text{O}_5$  catalysts the  $T_{50}$  temperature was now 520 °C, 36 °C lower than over the  $\text{V}_2\text{O}_5/\text{Al}_2\text{O}_3\text{-TiO}_2$  catalyst (Table 4).

#### 3.4. Selectivity

The PCE oxidation results with detected side products and calculated carbon balance over all the active phases supported with  $\text{Al}_2\text{O}_3\text{-CeO}_2$  are presented in Fig. 6a–d. The HCl yields during the PCE oxidation over all the catalysts are plotted in Fig. 7a–c.

Analysis of the reaction products confirmed that the main oxidation products in PCE oxidation in moist conditions over the tested catalysts are  $\text{CO}_2$  and HCl. Depending on the catalysts, carbon monoxide (CO) and traces of trichloroethylene (TCE,  $\text{C}_2\text{HCl}_3$ ),

chloroform (TCM,  $\text{CHCl}_3$ ) and ethylene ( $\text{C}_2\text{H}_4$ ) were detected during the light-off tests at lower temperature regions (Fig. 6). Over the  $\text{Pt}/\text{Al}_2\text{O}_3\text{-CeO}_2$  and  $\text{Pd}/\text{Al}_2\text{O}_3$  catalysts and below 420 °C the maximum values of 7 ppm and 8 ppm for TCE were observed, respectively. Over all the Rh catalysts traces of TCM were seen at the temperature lower than 400 °C; the highest detected TCM concentration was 5 ppm over  $\text{Rh}/\text{Al}_2\text{O}_3\text{-CeO}_2$  (Fig. 6c). Some ethylene formation was seen over all the Pd and  $\text{V}_2\text{O}_5$  catalysts and the maximum detected value of ethylene was 12 ppm at 500 °C over  $\text{Pd}/\text{Al}_2\text{O}_3\text{-CeO}_2$  (Fig. 6b). Ethylene formation was always seen at higher temperatures, with the Pd catalysts from 450 °C to 550 °C and with the  $\text{V}_2\text{O}_5$  catalysts from 430 °C to 600 °C. Above  $T_{90}$  over the Pt, Pd and Rh catalysts and also over all three tested supports (at any temperature) the only oxidation products detected were  $\text{CO}_2$ , CO and HCl.

Some carbon monoxide formation was detected with all but the  $\text{Pt}/\text{Al}_2\text{O}_3\text{-CeO}_2$  catalyst (Fig. 6a), however over the  $\text{V}_2\text{O}_5$  catalysts the CO formation was the most pronounced and the highest measured amount (243 ppm) was observed with  $\text{V}_2\text{O}_5/\text{Al}_2\text{O}_3\text{-CeO}_2$  at 571 °C (Fig. 6d). (At the same time  $\text{V}_2\text{O}_5/\text{Al}_2\text{O}_3\text{-CeO}_2$  was the most active vanadium catalyst with maximum of 89% PCE conversion.) With the Rh catalysts the maximum CO concentration was observed in the temperature range of 500 °C and 600 °C, e.g. over  $\text{Rh}/\text{Al}_2\text{O}_3\text{-TiO}_2$  the maximum CO concentration of 23 ppm was observed at 525 °C. In general, CO formation started above 430 °C and the selectivity was improved when temperature was increased as can be expected.

The differences in HCl yields over different supports can be seen in Fig. 7a–c.  $\text{Al}_2\text{O}_3\text{-CeO}_2$  and  $\text{Al}_2\text{O}_3\text{-TiO}_2$  showed higher HCl selectivity than  $\text{Al}_2\text{O}_3$ . Now, the HCl yields were reasonably high reaching up to 93% with  $\text{Pd}/\text{Al}_2\text{O}_3\text{-CeO}_2$  and up to 91% with  $\text{Pt}/\text{Al}_2\text{O}_3\text{-CeO}_2$ . With the same metals supported on  $\text{Al}_2\text{O}_3\text{-TiO}_2$  the HCl yield was reduced below 90%. The chlorine balance was not reached and therefore, it can be assumed that the rest of chlorides are in the form of  $\text{Cl}_2$  or stay as chlorides at the catalyst surface since only traces of other chlorinated by-products were detected during the light-off tests (and none at higher temperatures).

#### 4. Discussion

In the case of total oxidation of chlorinated compounds the high activity is not enough, high demands are also set to the selectivity of the catalyst. Introduction of a hydrogen source into the reaction stream is of special importance in order to avoid the formation of unwanted  $\text{Cl}_2$ . Both HCl selectivity and PCE oxidation activity were improved with an increased water amount in the feed, selectivity clearly more than activity (Fig. 4). From different water concentrations tested, 1.5 wt-% was chosen to be the amount in all the activity tests completed in this study, since above 1.6 wt-% of water the oxidation was enhanced only slightly and the disadvantages, such as unsteady  $\text{H}_2\text{O}$  evaporation and increased interference to the FTIR measurement due to larger water spectrum covering the characteristic peaks of the other compounds appeared.

The tested supports (without active phase) were quite active in PCE oxidation when compared to thermal experiments (see the PCE conversion curve from thermal tests in the Fig. 4 in our previous study [24]). Furthermore, all supports showed surprisingly high selectivity towards  $\text{CO}_2$ , CO and HCl and no other by-products were detected during the light-off tests. The overall activity and selectivity order of supports was  $\text{Al}_2\text{O}_3\text{-CeO}_2 > \text{Al}_2\text{O}_3\text{-TiO}_2 > \text{Al}_2\text{O}_3$  (Figs. 5 and 7). It looks like ceria as a thermal and structural stabilizer with its unique redox properties [35–39] is beneficial in PCE oxidation. Based on the characterizations, one clear difference between the supports is that besides 7.5 nm mesopores also smaller, 3.6 nm mesopores exist in the ceria-doped alumina. Over

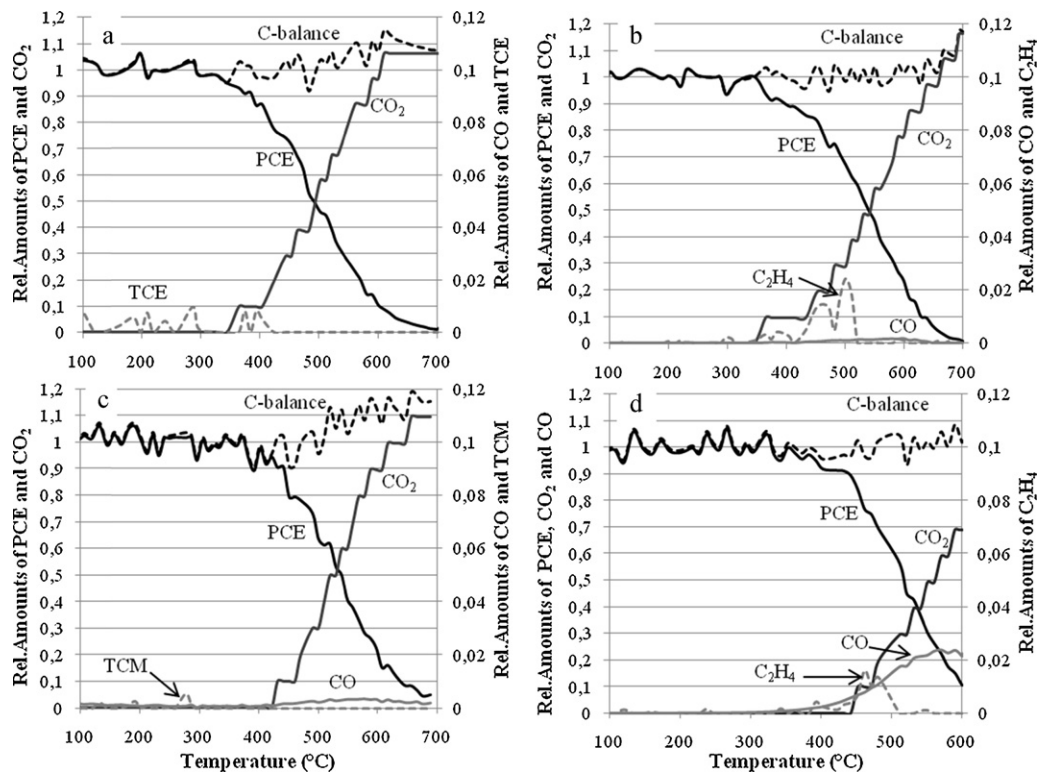


**Fig. 6.** PCE oxidation over (a) Pt, (b) Pd, (c) Rh and (d)  $V_2O_5$  catalysts supported on  $Al_2O_3$ - $CeO_2$  (the same conditions as in Fig. 5).

alumina and alumina-titania supports only monodispersed pore-sizes exist as the pore sizes are 7.7 nm and 7.8 nm, respectively (Fig. 1b, Table 2). This might have an advantage in the PCE oxidation but to confirm this, further testing of the pore-size effect would be needed.

The active materials used in this study were Pt, Pd, Rh and  $V_2O_5$  (Table 1) and as expected the addition of active phase to the catalyst showed considerable enhancement in catalysts performance, both in activity and selectivity (Figs. 5 and 7, Table 4). The activity and selectivity of the  $Al_2O_3$  supported catalysts were relatively low; the highest PCE conversion of 91% and the highest HCl yield of 80% were reached with the Rh/ $Al_2O_3$  catalyst at 688 °C. Almost all the  $Al_2O_3$ - $CeO_2$  and  $Al_2O_3$ - $TiO_2$  supported catalysts showed higher activity and HCl selectivity than the  $Al_2O_3$  supported catalysts, only exception was the titania-doped Pt catalysts as the activity and selectivity remained the same. Therefore, the discussion next is considering the changes as a result of the addition of 26 wt-%  $TiO_2$  or 23 wt-%  $CeO_2$  (Table 3) over all catalysts.

When the Pt catalysts are considered the activity order of the supports was  $Al_2O_3$ - $CeO_2$  >  $Al_2O_3$ - $TiO_2$  >  $Al_2O_3$ . This result is in line with the maximum rate of oxygen activation temperatures measured over the Pt catalysts showing that the activity of the Pt catalysts in PCE oxidation is related to the oxygen activation activity (see Section 3.1). Since the oxygen activation tests were carried out only over the Pt catalysts at this point, conclusions between the other active phases could not be done based on these results. The addition of 23 wt-% ceria improved the catalyst activity among all the active phases but the biggest improvement in activity due to  $CeO_2$  addition was seen with the Pt catalyst (Fig. 5). When the  $Pt/Al_2O_3$ - $CeO_2$  catalyst is compared to the  $Pt/Al_2O_3$  catalyst, the  $T_{50}$  temperature was degreased substantially, 93 °C from 585 °C to 492 °C and the maximum PCE conversion detected increased from 85% to 99% (Tables 4 and 5). Also the selectivity towards HCl was considerably improved as the second highest HCl yield, 91% was

detected. From all the 15 tested catalysts the  $Pt/Al_2O_3$ - $CeO_2$  catalyst was the only one which did not show any CO formation (Fig. 6a), but then it was the only Pt catalyst that showed traces of TCE formation ( $\leq 7$  ppm) under 430 °C (Fig. 6a). (The Pd/ $Al_2O_3$  catalyst was the other catalyst that showed any TCE formation.) Addition of 26 wt-% titania had only a small effect on the activity of the Pt catalyst and on its HCl yield when compared to the  $Pt/Al_2O_3$  catalyst. When the characterization results of the  $Pt/Al_2O_3$ - $CeO_2$  catalyst are compared to the results of the  $Pt/Al_2O_3$ - $TiO_2$  and  $Pt/Al_2O_3$  catalysts, besides the bidispersed pore-size present in the alumina-ceria support (Table 2), the Pt metal dispersions were 30% smaller, as the dispersions were now 35.5%, 49.8% and 49.4%, respectively (Table 1). This indicates that PCE oxidation is a structure sensitive reaction promoted on a larger Pt particle size increasing the density of reactive Pt-O species [24,38]. Shyu and Otto [40] reported a strong interaction between Pt and ceria as they studied Pt supported on alumina, ceria and ceria-alumina. The presence of noble metal has been reported to enhance the redox behavior of  $CeO_2$  [35,41–44] but also ceria has been reported to promote the reduction of noble metals [43–45]. Abbasi et al. [43] studied 1 wt-%  $Pt/Al_2O_3$ - $CeO_2$  catalysts with ceria loadings of 10, 20 and 30% in the oxidation of VOCs and found that the catalyst with the highest ceria loading (30%) was the most active in toluene oxidation. From the TPR analysis they saw that adding 1 wt-% platinum increased reducibility of the support but also ceria had a promoting effect on reducibility of Pt and  $Al_2O_3$ ; therefore they concluded that this mutual interaction leads to a more active catalyst for the oxidation of VOCs. Carlsson and Skoglund [46] concluded in their study that the significant increase in activity in the oxidation of carbon monoxide and methane over ceria-supported Pt is due to highly active sites at the platinum-ceria boundary but also, to some extent to the oxygen storage and release function and dynamics of the transport of oxygen in the  $Pt/CeO_2$  system. The strong synergistic effect between metal and support together with improved redox properties might be

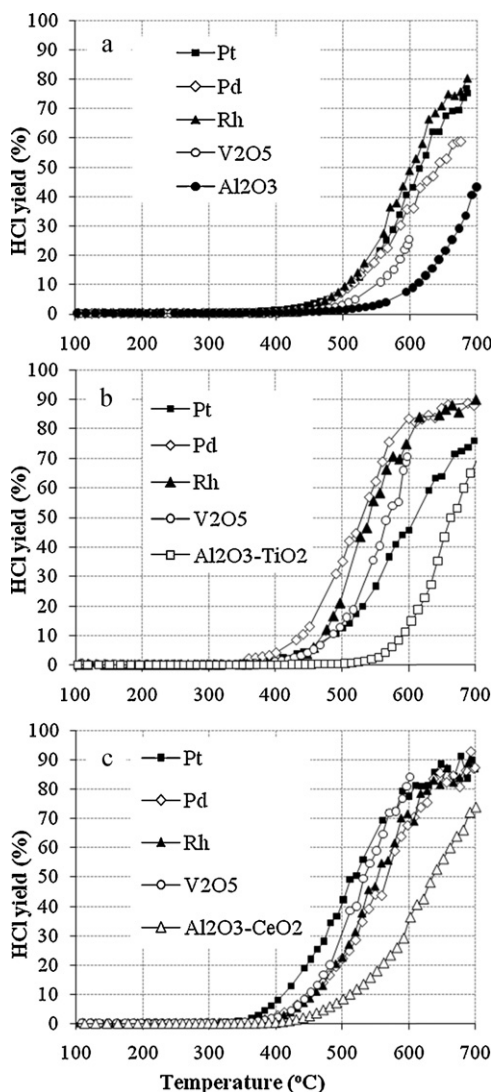


**Fig. 7.** The HCl yields over all (a)  $\text{Al}_2\text{O}_3$  (b)  $\text{Al}_2\text{O}_3\text{-TiO}_2$  and (c)  $\text{Al}_2\text{O}_3\text{-CeO}_2$  catalysts (the same conditions as in Fig. 5).

explanations for higher catalytic activity of the  $\text{Pt}/\text{Al}_2\text{O}_3\text{-CeO}_2$  catalyst in this study.

Over the Pd catalysts the activity order of supports was  $\text{Al}_2\text{O}_3\text{-TiO}_2 > \text{Al}_2\text{O}_3\text{-CeO}_2 > \text{Al}_2\text{O}_3$ . When 26 wt-%  $\text{TiO}_2$  was introduced to the support the activity of all active phases but Pt (see above) was notably enhanced. Over the  $\text{Pd}/\text{Al}_2\text{O}_3\text{-TiO}_2$  catalyst the  $T_{50}$  temperature was lowered considerably by 95 °C from 605 °C to 510 °C when compared to the alumina supported catalyst (Fig. 5, Table 4). The maximum PCE conversion was now 98% as over  $\text{Pd}/\text{Al}_2\text{O}_3$  it was 72%. Also the selectivity was remarkably enhanced by the addition of titania as the maximum HCl yield increased from 68% to 88% (Fig. 7). Over the  $\text{Pd}/\text{Al}_2\text{O}_3$  catalyst the maximum value of 8 ppm of TCE was detected below 420 °C. Some ethylene formation was seen over all the Pd catalysts and the maximum detected value of ethylene was 12 ppm at 500 °C over  $\text{Pd}/\text{Al}_2\text{O}_3\text{-CeO}_2$ . The enhancement noticed in the PCE oxidation activity over the titania-doped catalyst might be due to palladium being more easily reduced on  $\text{TiO}_2$  than on  $\text{Al}_2\text{O}_3$  as reported by Macleod et al. [47,48]. They concluded in their study that over  $\text{Pd}/\text{TiO}_2/\text{Al}_2\text{O}_3$  catalysts the synergy between alumina and titania derives from intrinsic surface chemistry of pure oxides and not from mixed oxide formation [48]. Also 23 wt-% of  $\text{CeO}_2$  improved the activity and selectivity of the Pd catalyst. When compared to  $\text{Al}_2\text{O}_3$  supported catalysts the  $T_{50}$  temperature was

lowered by 66 °C from 605 °C to 539 °C (Table 4) and the maximum HCl yield increased from 68% to 93% (Fig. 7). Chemisorption showed an increase in the Pd dispersion over the cerium-doped catalyst when compared to the alumina supported Pd catalyst. Besides a higher Pd dispersion other reasons for improved performance might be the properties of storing and releasing oxygen (redox properties) of ceria and the high lability of the lattice oxygen which are among the most important factors contributing to the catalytic reactivity of  $\text{CeO}_2$  in oxidation reactions [35]. Similar characteristic than over Pt and ceria interactions have been reported also over Pd and ceria [35,46,49–51]. Shyu et al. [50] found in their studies that  $\text{CeO}_2$  promotes oxidation of Pd to  $\text{PdO}$  both with and without alumina. Padilla et al. [51] studied 0.5 wt-%  $\text{Pd}/\text{Al}_2\text{O}_3$ -ceria catalysts and saw at higher cerium contents (5 and 10 wt-%) a characteristic oxidation-reduction cycle of cerium serving as the oxygen source and allowing  $\text{Pd}^0$  and  $\text{PdO}$  to co-exist and thus favoring benzene combustion. They also observed better stability over these catalysts and explained it by the effect of  $\text{CeO}_2$  which inhibited the deposition of carbonaceous species on the Pd surface.

With the Rh catalysts the activity order of supports was  $\text{Al}_2\text{O}_3\text{-TiO}_2 > \text{Al}_2\text{O}_3\text{-CeO}_2 > \text{Al}_2\text{O}_3$ , the same as above over Pd. However, with Rh the improvement in performance resulting from titania or ceria addition was not as noticeable as it was with Pt and Pd seen earlier. One reason is that already the  $\text{Rh}/\text{Al}_2\text{O}_3$  catalyst showed high activity and HCl selectivity as from all alumina supported catalysts the  $T_{50}$  temperature of the Rh catalyst was the lowest (560 °C) (Table 4) and both, the PCE conversion and the maximum HCl yield were the highest, 91% and 80%, respectively (Fig. 7). The addition of 26 wt-%  $\text{TiO}_2$  to the support lowered the  $T_{50}$  temperature by 38 °C and increased the HCl yield by 8%. In the CO and  $\text{CO}_2$  formation there was a small deterioration. Addition of 23 wt-%  $\text{CeO}_2$  affected the PCE oxidation activity and HCl selectivity even less than titania did, but the CO and  $\text{CO}_2$  formation was somewhat improved if compared to the alumina supported Rh catalyst. Traces of TCM were seen below 400 °C over all the Rh catalysts, the maximum detected value was 5 ppm over  $\text{Rh}/\text{Al}_2\text{O}_3\text{-CeO}_2$ . Over all the Rh catalysts high surface areas from  $163 \text{ m}^2 \text{ g}^{-1}$  to  $170 \text{ m}^2 \text{ g}^{-1}$  were observed and the addition of both, titania and ceria increased the Rh dispersion markedly. The dispersion over titania-doped catalysts was now 61% as over alumina based Rh catalyst it was 29% (Table 1) indicating that PCE oxidation is sensitive to the Rh particle size, i.e. smaller particles are more active than the bigger ones. (Over  $\text{Al}_2\text{O}_3\text{-CeO}_2$  the Rh dispersion seen was even higher, 74.9%.) Santos et al. [52] came to the same conclusion when they observed an enhancement in ethanol oxidation activity over  $\text{Rh}/\text{TiO}_2$  catalyst as the particle size of Rh decreased. These together with the supposed strong metal-support interaction (SMSI<sup>1</sup>) between active metal and  $\text{TiO}_2$  support, which e.g. increases the amount of activated oxygen, may be responsible for the enhanced activity of the  $\text{Rh}/\text{Al}_2\text{O}_3\text{-TiO}_2$  catalyst [53–57].

The activity order of supports over the  $\text{V}_2\text{O}_5$  catalysts was  $\text{Al}_2\text{O}_3\text{-CeO}_2 > \text{Al}_2\text{O}_3\text{-TiO}_2 > \text{Al}_2\text{O}_3$ , the same as over the supports (without any active phase) and the Pt catalysts described above. The addition of both ceria and titania improved the activity of  $\text{V}_2\text{O}_5$  catalysts a great deal, the  $T_{50}$  temperature was degreased from above 600 °C (with the  $\text{V}_2\text{O}_5/\text{Al}_2\text{O}_3$  at 597 °C the conversion reached was 35%, NB: the maximum temperature of the tests was now 600 °C) down to 556 °C and 520 °C, respectively. Also the HCl selectivity was enhanced over ceria or titania-doped catalysts as the maximum HCl yields detected increased from 24% to 84% and 70%, respectively. Some carbon monoxide formation was detected with all the

<sup>1</sup> SMSI means a change in catalytic behaviour due to interactions between metal and non-metallic support. Two main mechanisms proposed are charge transfer (reduction of support material), or encapsulation of metal clusters by support material [52,53].

catalysts (except with Pt/Al<sub>2</sub>O<sub>3</sub>-CeO<sub>2</sub>) but overall the V<sub>2</sub>O<sub>5</sub> catalysts the CO concentrations detected were high when compared to other supported catalysts. The highest CO<sub>2</sub> concentration among V<sub>2</sub>O<sub>5</sub> catalysts was detected over the Al<sub>2</sub>O<sub>3</sub>-TiO<sub>2</sub> support, the second highest over the Al<sub>2</sub>O<sub>3</sub>-CeO<sub>2</sub> support. Some ethylene formation ( $\leq 12$  ppm) was seen over the V<sub>2</sub>O<sub>5</sub> catalysts from 430 °C to 600 °C. Over the V<sub>2</sub>O<sub>5</sub>/Al<sub>2</sub>O<sub>3</sub>-CeO<sub>2</sub> catalyst the oxide-support interaction and redox properties of both vanadium and cerium seem to be advantageous in PCE oxidation [35–37,58–60]. The improved activity of the titania-doped catalyst when compared to the alumina supported catalyst might be due to higher population of tetrahedrally coordinated vanadium species resulting in lower reduction temperature, but also because of the possibly high dispersion of vanadium on the titania surface governed by the difference in surface free energy as seen in the literature [61,62]. Since the V<sub>2</sub>O<sub>5</sub> dispersion was not measured this cannot be confirmed in our study. Krisnamoorthy et al. [63,64] studied the catalytic oxidation of 1,2-dichlorobenzene (o-DCB) and found that V<sub>2</sub>O<sub>5</sub>/Al<sub>2</sub>O<sub>3</sub> catalysts were less active and selective than V<sub>2</sub>O<sub>5</sub>/TiO<sub>2</sub> catalysts. Based on their turnover (TOF) calculations they suggested that contrary to SCR, only a single vanadia site (surface redox site) participates in the rate-determining steps of o-DCB oxidation.

In general, the CO formation started above 430 °C and as expected the selectivity towards CO<sub>2</sub> was improved when the temperature was increased. The CO formation was significantly decreased by the introduction of Pt, Pd and Rh over all the supports, and the lowest CO formation was seen over the Al<sub>2</sub>O<sub>3</sub>-CeO<sub>2</sub> supported catalysts. High activities and selectivities (high HCl yields and low CO concentrations) were also achieved over Pd and Rh supported on Al<sub>2</sub>O<sub>3</sub>-TiO<sub>2</sub>. If compared to our previous study [24] it seems that the higher Pt and Pd loadings (now ~1 wt-% Pt and ~0.5 wt-% Pd loadings in comparison with 0.22 wt-% Pt and Pd and 0.42 wt-% Pt loadings) noticeably enhanced the selectivity; the maximum HCl yield seen then was 57% at 720 °C over 0.23 wt-% Pt/Al<sub>2</sub>O<sub>3</sub>-CeO<sub>2</sub>-zeolite catalyst and now in this study the maximum HCl yield detected was 93% at 693 °C over the 0.61 wt-% Pd/Al<sub>2</sub>O<sub>3</sub>-CeO<sub>2</sub> catalyst.

Depending on the catalysts, besides carbon monoxide, traces of trichloroethylene (TCE, C<sub>2</sub>HCl<sub>3</sub>), chloroform (TCM, CHCl<sub>3</sub>) and ethylene (C<sub>2</sub>H<sub>4</sub>) were detected during the light-off tests at lower temperature regions. These by-products can be assumed to be partially oxidized PCE compounds escaping from the catalyst surface before the total oxidation. Since detected chlorinated by-products were present only in small quantities (and none at higher temperatures) it can be assumed that the rest of chlorides are in the form of Cl<sub>2</sub> or stay as chlorides at the catalyst surface. From IC measurements it was seen that after the activity tests the catalysts contained water soluble chlorine from 2.7 to 4.9 mg g<sup>-1</sup>. Neither the decrease in surface area nor chlorine residual was found to affect the activity of the catalysts during these experiments. Based on the carbon balance over Pt, Pd, Rh and V<sub>2</sub>O<sub>5</sub> over Al<sub>2</sub>O<sub>3</sub>-CeO<sub>2</sub> catalysts (Fig. 6) there is no coke formation expected in PCE oxidation with these catalysts, but to ensure this and to see the long term chlorine effect over the catalysts, more tests and characterizations over these catalysts are under study and will be reported soon.

## 5. Conclusions

Totally 15 metallic monoliths with four different active phases (Pt, Pd, Rh and V<sub>2</sub>O<sub>5</sub>) supported on Al<sub>2</sub>O<sub>3</sub>, Al<sub>2</sub>O<sub>3</sub>-TiO<sub>2</sub> and Al<sub>2</sub>O<sub>3</sub>-CeO<sub>2</sub> were examined in the oxidation of PCE. In summary the following results are highlighted:

- The amount of water as a hydrogen source was optimized to be 1.5 wt-% by testing the effect of water content on the PCE oxidation activity and HCl yield at 600 °C. Over the Pt/Al<sub>2</sub>O<sub>3</sub>-CeO<sub>2</sub> catalyst water greatly improved the selectivity towards HCl formation (22%) and also a small enhancement in the PCE conversion was seen (7%).
- All supports (Al<sub>2</sub>O<sub>3</sub>, Al<sub>2</sub>O<sub>3</sub>-TiO<sub>2</sub> and Al<sub>2</sub>O<sub>3</sub>-CeO<sub>2</sub>) showed activity in PCE oxidation, but the detected selectivity was unexpected, only CO<sub>2</sub>, CO and HCl were seen in the product stream.
- The nature of the support affected strongly the activity and selectivity of the catalysts as the introduction of TiO<sub>2</sub> or CeO<sub>2</sub> into Al<sub>2</sub>O<sub>3</sub> made these supports superior in comparison to pure Al<sub>2</sub>O<sub>3</sub> (only exception was the titania-doped Pt catalysts as the activity and selectivity remained the same). It seems that over the oxidation of PCE the redox properties and the amount of activated oxygen play a big role.
- Of all the catalysts tested, Pt/Al<sub>2</sub>O<sub>3</sub>-CeO<sub>2</sub> showed the highest activity and the second highest HCl selectivity as the PCE conversion reached 99% at 688 °C and the maximum HCl yield was 91%. The second best catalyst was the Pd/Al<sub>2</sub>O<sub>3</sub>-CeO<sub>2</sub> catalyst with 99% PCE conversion at 693 °C and the highest of all maximum HCl yield of 93%.
- When compared to our previous study [24] the HCl yields were noticeably enhanced in this study most likely due to higher active metal loadings (now ~1 wt-% Pt and ~0.5 wt-% Pd loadings in comparison with 0.22 wt-% Pt and Pd and 0.42 wt-% Pt loadings).
- Also Rh catalysts showed high activity: Rh/Al<sub>2</sub>O<sub>3</sub> catalyst was the most active from all alumina supported catalysts. However, when titania or ceria was added into the alumina support, the activity and selectivity was improved even further. Besides increased Rh dispersion indicating that PCE oxidation is sensitive to the Rh particle size, i.e. smaller particles are more active than the bigger ones, also the supposed strong metal-support interaction between active metal and TiO<sub>2</sub> support, which e.g. increases the amount of activated oxygen, may be responsible for the enhanced activity of the Rh/Al<sub>2</sub>O<sub>3</sub>-TiO<sub>2</sub> catalyst.
- The addition of TiO<sub>2</sub> or CeO<sub>2</sub> into Al<sub>2</sub>O<sub>3</sub> enhanced the performance of the V<sub>2</sub>O<sub>5</sub> catalysts as the maximum PCE conversion was increased from 35% to 77% and 89%, respectively. Over the V<sub>2</sub>O<sub>5</sub>/Al<sub>2</sub>O<sub>3</sub>-CeO<sub>2</sub> catalyst the oxide-support interaction and redox properties of both vanadium and cerium seem to be advantageous in PCE oxidation. The improved activity of the titania-doped catalyst might be due to higher population of tetrahedrally coordinated vanadium species resulting to lower reduction temperature, but also because of the possibly higher dispersion of vanadium on the titania surface governed by the difference in surface free energy as seen in the literature.
- Depending on the catalysts, carbon monoxide and traces of trichloroethylene, chloroform and ethylene were detected during the light-off tests at lower temperature regions. These by-products can be assumed to be partially oxidized PCE compounds escaping from the catalyst surface before the total oxidation. Above T<sub>90</sub> over the Pt, Pd and Rh catalysts the only oxidation products detected were CO<sub>2</sub>, CO and HCl.

## Acknowledgements

This work has been carried out with the financial support of the Council of Oulu region from European Regional Development Fund and the City of Oulu. Mr. Jorma Penttinen, Prof. Ulla Lassi and Mrs. Tiina Laitinen are acknowledged for their contribution to the experimental work. Mr. Zdeněk Matěj from the Charles University in Prague and Doc. Libor Čapek from the University of Pardubice are appreciated for their kind contribution for XRD and UV-vis characterizations. Dr. Nicolas Bion and Dr. Daniel Duprez from the

University of Poitiers; France are acknowledged for their collaboration related to the isotopic experiments.

## References

- [1] Euro Chlor, [http://www.eurochlor.org/chlorinated-solvents-\(ecsa\)/about-chlorinated-solvents/facts-figures.aspx](http://www.eurochlor.org/chlorinated-solvents-(ecsa)/about-chlorinated-solvents/facts-figures.aspx) (accessed November 2011).
- [2] S.E. Manahan, Environmental Chemistry, fifth ed., Lewis Publishers, Michigan, 1991.
- [3] International Chemical Safety Cards (ICSC), <http://www.ilo.org/legacy/english/protection/safework/cis/products/icsc/dtasht/index.htm> (accessed July 2011).
- [4] DIRECTIVE 2010/75/EU, Off. J. Eur. Communities, <http://eur-lex.europa.eu/LexUriServ/Lex UriServ.do?uri=OJ:L:2010:334:0017:0119:EN:PDF> (accessed November 2011).
- [5] E.C. Moretti, Practical Solutions for Reducing Volatile Organic Compounds and Hazardous Air Pollutants, AIChE, New York, 2001.
- [6] K. Everaert, J. Baeyens, J. Hazard. Mater. B109 (2004) 113–139.
- [7] L.F. Liotta, Appl. Catal. B 100 (2010) 403–412.
- [8] R. López-Fonseca, J.I. Gutiérrez-Ortiz, J.R. González-Velasco, Catal. Commun. 5 (2004) 391–396.
- [9] G. Sinquin, C. Petit, S. Libs, J.P. Hindermann, A. Kiennemann, Appl. Catal. B 27 (2000) 105–115.
- [10] R. López-Fonseca, S. Cibrián, J.I. Gutiérrez-Ortiz, M.-A. Gutiérrez-Ortiz, J.R. González-Velasco, AIChE J. 49 (2) (2003) 496–504.
- [11] A. Koyer-Golkowska, A. Musialik-Piotrowska, J.D. Rutkowski, Catal. Today 90 (2004) 133–138.
- [12] J.R. González-Velasco, A. Aranzabal, R. López-Fonseca, R. Ferret, J.A. González-Marcos, Appl. Catal. B 24 (2000) 33–43.
- [13] J.R. González-Velasco, A. Aranzabal, J.I. Gutiérrez-Ortiz, R. López-Fonseca, M.A. Gutiérrez-Ortiz, Appl. Catal. B 19 (1998) 189–197.
- [14] J. Corella, J.M. Toledo, A.M. Padilla, Appl. Catal. B 27 (2000) 243–256.
- [15] A. Musialik-Piotrowska, K. Syczewska, Catal. Today 73 (2002) 333–342.
- [16] B. Chen, C. Bai, R. Cook, J. Wright, C. Wang, Catal. Today 30 (1996) 15–20.
- [17] A.M. Padilla, J. Corella, J.M. Toledo, Appl. Catal. B 22 (1999) 107–121.
- [18] H. Windawi, Z.C. Zhang, Catal. Today 30 (1996) 99–105.
- [19] S.D. Yim, K-H. Chang, D.J. Koh, I-S. Nam, Y.G. Kim, Catal. Today 63 (2000) 215–222.
- [20] S.D. Yim, D.J. Koh, I.-S. Nam, Catal. Today 75 (2002) 269–276.
- [21] P.S. Chintawar, H.L. Greene, Appl. Catal. B 13 (1997) 81–92.
- [22] R.W. Van den Brink, P. Mulder, R. Louw, G. Sinquin, C. Petit, J.-P. Hindermann, J. Catal. 180 (1998) 153–160.
- [23] R.M. Alberici, M.A. Mendes, W.F. Jardim, M.N. Eberlin, J. Am. Soc. Mass Spectrom. 9 (1998) 1321–1327.
- [24] S. Pitkäaho, S. Ojala, T. Maunula, A. Savimäki, T. Kinnunen, R.L. Keiski, Appl. Catal. B 102 (2011) 395–403.
- [25] P. Scardi, M. Leoni, Acta Crystallogr. Sect. A 58 (2002) 190–200.
- [26] Z. Matěj, R. Kužel, L. Nichtová, Powder Diffr. 25 (2010) 125–131.
- [27] L. Čapek, R. Bulánek, J. Adam, L. Smoláková, H. Sheng-Yang, P. Čičmanec, Catal. Today 141 (2009) 282–287.
- [28] R. Bulánek, L. Čapek, M. Setnicka, P. Cicmanek, J. Phys. Chem. C 115 (2011) 12430–12438.
- [29] S. Lowell, J.E. Shields, M.A. Thomas, M. Thommes, Characterization of Porous Solids and Powders: Surface Area, Pore Size and Density, Springer, Netherlands, 2006.
- [30] R.-S. Zhou, R.L. Snyder, Acta Crystallogr. Sect. B 47 (1991) 617–630.
- [31] F. Klose, T. Wolff, H. Lorenz, A. Seidel-Morgenstern, Y. Suchorski, M. Piórkowska, H. Weiss, J. Catal. 247 (2007) 176–193.
- [32] F. Arena, F. Frusteri, A. Parmaliana, Appl. Catal. B 176 (1999) 189–199.
- [33] J. Haber, Catal. Today 142 (2009) 100–113.
- [34] D. Duprez, Isotopes in Heterogeneous Catalysis, Catalytic Science Series, vol. 4, Imperial College Press, London, 2006.
- [35] A. Trovarelli, Catal. Rev. 38 (1996) 439–520.
- [36] A. Holmgren, B. Andersson, D. Duprez, Appl. Catal. B 22 (1999) 215–230.
- [37] A. Piras, A. Trovarelli, G. Dolcetti, Appl. Catal. B 28 (2000) L77–L81.
- [38] T.F. Garetto, C.R. Pesteguía, Appl. Catal. B 32 (2001) 83–94.
- [39] J.I. Gutiérrez-Ortiz, B. de Rivas, R. López-Fonseca, J.R. González-Velasco, Appl. Catal. B 65 (2006) 191–200.
- [40] J.Z. Shyu, K. Otto, J. Catal. 115 (1989) 16–23.
- [41] L. Pino, A. Vita, M. Cordaro, V. Recupero, M.S. Hedge, Appl. Catal. A 243 (2003) 135–146.
- [42] S. Damyanova, J.M.C. Bueno, Appl. Catal. A 253 (2003) 135–150.
- [43] Z. Abbasi, M. Haghghi, E. Fatehifar, S. Saedy, J. Hazard. Mater. 186 (2011) 1445–1454.
- [44] R. Ramírez-López, I. Elizalde-Martinez, L. Balderas-Tapia, Catal. Today 150 (2010) 358–362.
- [45] A.C.S.F. Santos, S. Damyanova, G.N.R. Texeira, L.V. Mattos, F.B. Noronha, F.B. Passos, J.M.C. Bueno, Appl. Catal. A 205 (2005) 123–132.
- [46] P.-A. Carlsson, M. Skoglund, Appl. Catal. B 101 (2011) 669–675.
- [47] N. Macleod, R. Cropley, R.M. Lambert, Catal. Lett. 86 (2003) 69–75.
- [48] N. Macleod, R. Cropley, J.M. Keel, R.M. Lambert, J. Catal. 221 (2004) 20–31.
- [49] M. Haneda, T. Mizushima, N. Kakuta, J. Phys. Chem. B 102 (1998) 6579–6587.
- [50] J.Z. Shyu, K. Otto, W.L.H. Watkins, G.W. Graham, R.K. Belitz, H.S. Gandhi, J. Catal. 114 (1988) 23–33.
- [51] J.M. Padilla, G. Del Angel, J. Navarrete, Catal. Today 133–135 (2008) 541–547.
- [52] V.P. Santos, S.A.C. Carabineiro, P.B. Tavares, M.F.R. Pereira, J.J.M. Órfão, J.L. Figueiredo, Appl. Catal. B 99 (2010) 198–205.
- [53] S.J. Tauster, S.C. Fung, R.L. Garten, J. Am. Chem. Soc. 100 (1978) 170–175.
- [54] Ch. Linsmeier, H. Knözinger, E. Taglauer, Nucl. Instrum. Methods Phys. Res. B 118 (1996) 533–540.
- [55] Ch. Linsmeier, E. Taglauer, Appl. Catal. A 391 (2011) 175–186.
- [56] Q. Li, K. Wang, S. Zhang, M. Zhang, J. Yang, Z. Jin, J. Mol. Catal. A: Chem. 258 (2006) 83–88.
- [57] L. Mao, Q. Li, Z. Zhang, Solar Energy 81 (2007) 1280–1284.
- [58] S. Colussi, C. de Leitenburg, G. Dolcetti, A. Trovarelli, J. Alloys Compd. 374 (2004) 387–392.
- [59] M. Ozawa, M. Hattori, T. Yamaguchi, J. Alloys Compd. 451 (2008) 621–623.
- [60] J.P. Dunn, P.R. Koppula, H.G. Stenger, I.E. Wachs, Appl. Catal. B 19 (1998) 103–117.
- [61] J. Haber, T. Machej, T. Czepe, Surf. Sci. 151 (1985) 301–310.
- [62] M. Gasior, J. Haber, T. Machej, Appl. Catal. 33 (1987) 1–14.
- [63] S. Krishnamoorthy, J.B. Baker, M.D. Amiridis, Catal. Today 40 (1998) 39–46.
- [64] S. Krishnamoorthy, M.D. Amiridis, Catal. Today 51 (1999) 203–214.